

## Article

# Multifrequency Downstream Hydraulic Geometry of Alluvial Mountain Rivers Located on the Qinghai–Tibet Plateau

Chao Qin <sup>1,2,3</sup> , Baosheng Wu <sup>1,2,3</sup> , Yuan Xue <sup>1,2,3,\*</sup> , Xudong Fu <sup>1,2,3</sup>, Guangqian Wang <sup>1,2,3</sup> and Ge Wang <sup>1,2,3</sup>

<sup>1</sup> State Key Laboratory of Hydrosience and Engineering, Tsinghua University, Beijing 100084, China; glqinchao@nwsuaf.edu.cn (C.Q.); xdfu@tsinghua.edu.cn (X.F.); dhhwgq@mail.tsinghua.edu.cn (G.W.); wangg19@mails.tsinghua.edu.cn (G.W.)

<sup>2</sup> Key Laboratory of Hydrosphere Sciences of the Ministry of Water Resources, Tsinghua University, Beijing 100084, China

<sup>3</sup> Department of Hydraulic Engineering, Tsinghua University, Beijing 100084, China

\* Correspondence: xueyuan\_thu@163.com

**Abstract:** Downstream hydraulic geometry (DHG) for multiple discharge frequencies remains poorly investigated. This paper seeks to clarify the DHG relations of different discharge frequencies and proposes the definition, mathematical expression, and geomorphological interpretation of multifrequency DHG (MFDHG). It also verifies the existence of DHG and MFDHG in the six major exoreic rivers located in the Qinghai–Tibet Plateau. MFDHG can be depicted with (1) log-linear plots between DHG coefficients and exponents for multiple discharge frequencies and (2) independent DHG curves intersecting near congruent discharge, width, depth, or velocity. The results show that rivers in the study area exhibit strong DHG relations. The variations in the DHG coefficients and exponents usually exhibit opposite trends with increasing discharge frequency. The MFDHG of a river reach is generally stronger than that of a river basin. Congruent hydraulics, as indices of geometric variability and hydraulic self-similarity, reflect consistent changes in hydraulic variables downstream. MFDHG is a novel geomorphic phenomenon that bridges spatiotemporal dimensions in HG systems and provides a basis for establishing an overall HG relationship.

**Keywords:** multifrequency downstream hydraulic geometry MFDHG; discharge frequency; river network; Qinghai–Tibet Plateau



**Citation:** Qin, C.; Wu, B.; Xue, Y.; Fu, X.; Wang, G.; Wang, G.

Multifrequency Downstream Hydraulic Geometry of Alluvial Mountain Rivers Located on the Qinghai–Tibet Plateau. *Water* **2023**, *15*, 2139. <https://doi.org/10.3390/w15112139>

Academic Editors: Vlassios Hrissanthou, Bommanna Krishnappan, Mike Spiliotis and Konstantinos Kaffas

Received: 30 March 2023

Revised: 31 May 2023

Accepted: 1 June 2023

Published: 5 June 2023



**Copyright:** © 2023 by the authors. Licensee MDPI, Basel, Switzerland. This article is an open access article distributed under the terms and conditions of the Creative Commons Attribution (CC BY) license (<https://creativecommons.org/licenses/by/4.0/>).

## 1. Introduction

Empirical hydraulic geometry (HG) describes the quantitative relationship between river morphology (cross sections or longitudinal profiles) and basin characteristics. The relationships between discharge ( $Q$ ), river width ( $W$ ), average flow depth ( $H$ ), and flow velocity ( $V$ ) of an individual cross section are defined as At-a-station HG (AHG), while similar trends between  $Q$  and  $W$ ,  $H$ , and  $V$  among cross sections in the downstream direction are termed Downstream HG (DHG). Specifically, strong DHG relations have mostly been verified along river reaches. For different river systems, data from various watersheds with bankfull discharge were also combined to reveal good DHG relations between channel geometry and discharge [1].

An empirical engineering procedure for the design of unlined canals was developed by Lindley [2] early in the 20th century. This engineering procedure, from which HG was directly derived, was summarized by Leopold and Maddock [3] in the form of a power law in alluvial channels:

$$W = aQ^b \quad (1)$$

$$H = cQ^f \quad (2)$$

$$V = kQ^m \quad (3)$$

where  $a$ ,  $c$ , and  $k$  are the HG coefficients, and  $b$ ,  $f$ , and  $m$  are the HG exponents of rivers that conform to the regime theory.

Previous studies of HGs have primarily focused on their existence under various geomorphic conditions [4–7] and their theoretical bases [8–11], denotations and connotations [8,12,13], simulations [13,14], and applications. Although HG relations were treated as purely empirical, they were widely used for streamflow measurements and then for routing in hydrologic models [15,16], geomorphological assessment [10,11], river engineering and stream restoration [17–19], discharge estimation [12,20], and river carbon emissions [21,22].

Establishing an overall HG relationship is a challenging topic that has attracted much attention. The aims of this endeavor are (1) to build dimensionless analytical HG expressions, (2) to include as large an area as possible covering diverse boundary conditions in the spatial dimension, and (3) to simultaneously simulate variations between channel geometry and discharge along the length of the river and the water level in the spatiotemporal dimension. Consistent channel-bounding (bed and bank) material contributes to the constant variation between channel morphology and hydraulic variables; this has been emphasized through regime theory in many previous studies [1]. Dimensionless DHGs across morphologically similar sand beds [11] or gravel riverbeds [10] have been proposed to construct an overall HG relationship. Recent studies have injected fresh perspectives into classic HG studies. For instance, all anabranches of one cross section of a river with multiple channels can be plotted to yield an interchannel HG [23]. In the downstream direction, based on the idea that “cross sections of a given stream system are interrelated” [24], basin HG has been proposed to define the average values of hydraulic variables for a given streamflow and drainage area in a hydrologically homogeneous basin [8,25]. Furthermore, a specific cross section can be linked to the outlet of the river network by the same runoff event [26]. Local variations in cross sectional form are possible sources of scatter in DHG [18]. Therefore, relationships between the AHG of channels in a downstream direction are expected. At-Many-stations HG (AMHG) refers to the paired coefficients and exponents of AHG from many cross sections of a given river reach that are functionally related to one another and exhibit a log-linear relationship [27]. AMHG encompasses variations in both water levels (multiple discharge frequencies) and cross sections (multiple locations) [12]. It extends the spatial dimension from a single AHG cross section to strong relations across a whole river network. All these efforts pave the way for creating a possible overall HG relationship. More facets of HG than previously thought can be uncovered by closely linking DHG and AHG [28].

Previous DHG studies have usually considered bankfull discharge to be the formative discharge (channel-forming discharge); this highlights the dominant role of bankfull flow in shaping channel morphology, as it is the transition from shaping channels to shaping floodplains based on discharge and sediment load. However, a single discharge frequency cannot quantify the variations in hydraulic variables of individual cross sections. DHG exponents are significantly influenced by discharge frequencies [29]. From the limited data presented in Table 1, we find that when discharge frequencies varied from 2–50%, the differences in DHG width coefficients, and exponents changed sharply in the ranges of 13–69% and 32–375%, respectively. However, no universal trend in the variations in coefficients and exponents with changing discharges has been identified to date [30] (Table 1). Based on these facts and fresh perspectives on the classic HG topic, we will examine whether the change in DHG exponents with discharge frequency is a universal rule and whether the DHG coefficients regularly change with discharge frequency. AMHG depicts HG variations in both the spatial and temporal dimensions across river networks on the basin scale [7]. Similarly, we can hypothesize that a series of DHGs with multiple discharge frequencies will include as large an area as possible with similar boundary conditions on the basin scale.

**Table 1.** Values, maximum differences, and variation trends of DHG exponents at different discharge frequencies from the literature.

Country	References	Discharge Frequency/%	<i>a</i>	<i>b</i>	<i>f</i>	<i>m</i>	Maximum Difference/%				Variation Trend		
							<i>a</i>	<i>b</i>	<i>f</i>	<i>m</i>	<i>b</i>	<i>f</i>	<i>m</i>
US	[31]	50		0.34	0.45	0.32							
		15		0.38	0.42	0.32		32.4	7.1	88.2	increase	no trend	no trend
		2		0.45	0.43	0.17							
United Kingdom	[29]	50		0.46	0.16	0.38							
		15		0.54	0.23	0.23		32.6	93.8	375.0	increase	increase	decrease
		2		0.61	0.31	0.08							
Canada	[32]	83	5.6	0.51									
		50	4.8	0.53									
		20	3.8	0.54			68.5	5.4				increase	
		10	3.3	0.54									
Puerto Rico	[33]	70		0.46	0.27	0.27							
		50		0.44	0.30	0.35		4.5	18.5	40.0	no trend	increase	no trend
		30		0.46	0.32	0.25							

Thus, the key findings of previous DHG studies and the remaining gaps are summarized as follows: (1) discharge frequency significantly influences DHG coefficients and exponents, but research on its variation characteristics is lacking, and whether DHG coefficients and exponents are strongly correlated is unclear; and (2) to extract the common characteristics of existing HG relations, a combination of AHG and DHG features with spatiotemporal dimensions is necessary to contribute to the construction of an overall HG relationship. Due to the limitations of previous studies, this article aims to (1) explore relationships between DHG coefficients and exponents under multiple discharge frequencies; (2) identify any apparent trend in DHG coefficients and exponents based on changes in discharge frequencies; and (3) propose a framework system of multifrequency DHG (MFDHG) that may be the foundation of an overall HG relationship.

In Section 3, the definition and mathematical expression for MFDHG is proposed, along with its geomorphological interpretation along a river reach and for different reaches located in the same river basin based upon the hypothesis of the DHG series with multiple discharge frequencies. Then, we verify DHGs based on bankfull discharge and present MFDHGs in nine scenarios in river systems originating from the QTP in Sections 4.1 and 4.2. The typical methods for estimating bankfull discharge and fitting DHGs are presented in detail in Sections 2.2 and 2.3.

## 2. Data and Methods

### 2.1. Data and Study Area

#### 2.1.1. Study Area

The study area is located in the eastern and southern portions of the Qinghai–Tibet Plateau (QTP) and includes three national river basins (the upper Yellow River (YR), the Yalong River (YLR), and the upper Jinsha River (JSR), all of which flow to the Pacific Ocean) and three international river basins (the Lantsang River (LCR), which flows to the Pacific Ocean, and the Nu River (NR) and the Yarlung Zangbo River (YLZBR), which flow to the Indian Ocean) (Figure 1). The total area of the study area is  $130.787 \times 10^4$  km<sup>2</sup>. To maintain the integrity of the basins and expand the database, portions of the connecting regions between the QTP and the Loess Plateau, as well as the Yunnan–Kweichow Plateau, are included (Figure 1).

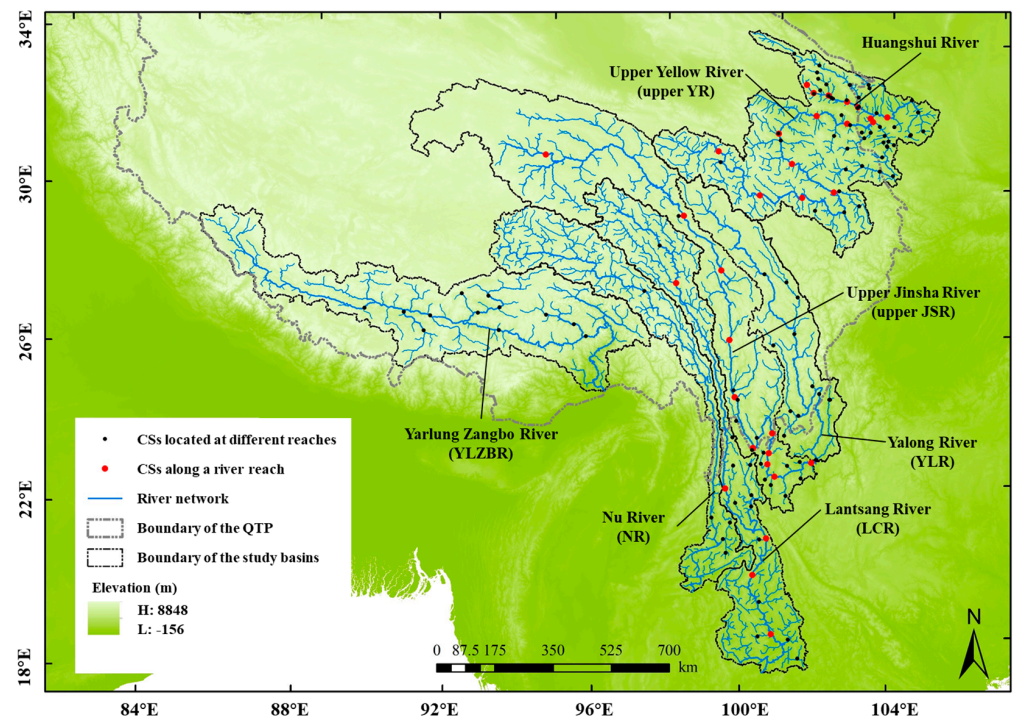


**Figure 1.** Location of the study area and cross sections (CSs). Red dots represent cross sections along a river reach (the 1st–4th scenarios of Table 2). Black dots represent cross sections located at different reaches of the same river basin (the 5th–9th scenarios of Table 2).

**Table 2.** DHG coefficients, exponents, and strength  $R^2$  of the six rivers and their tributaries originating from the QTP under bankfull conditions. DHG exponents of the theoretical solutions and the global rivers are presented for comparison with the data generated from the QTP. The  $a \times c \times k$  represents the product of DHG coefficients, while the  $b + f + m$  represents the sum of DHG exponents;  $R^2$  indicates the determination coefficient between discharges and river width/water depth/flow velocities under bankfull conditions.

Sources	Scenarios	Width-DHG			Depth-DHG			Velocity-DHG			Relations	
		<i>a</i>	<i>b</i>	$R^2$	<i>c</i>	<i>f</i>	$R^2$	<i>k</i>	<i>m</i>	$R^2$	$a \times c \times k$	$b + f + m$
Along a river reach	Main stream of the YR	35.62	0.22	0.54	0.12	0.48	0.86	0.24	0.30	0.65	1.00	1.00
	Main stream of the JSR	45.01	0.15	0.02	0.13	0.51	0.39	0.18	0.34	0.29	1.01	1.00
	Main stream of the LCR	0.11	0.88	0.76	0.13	0.50	0.57	77.66	-0.38	0.88	0.98	1.00
	Main stream of the Huangshui River	4.57	0.46	0.57	0.25	0.33	0.59	0.88	0.21	0.74	1.01	1.00
Different reaches located in the same river basin	Tributaries of the JSR	7.38	0.31	0.65	0.23	0.43	0.58	0.60	0.26	0.55	1.00	1.00
	Tributaries of the YLR	2.18	0.54	0.46	0.19	0.44	0.29	2.41	0.02	0.01	1.01	1.00
	Tributaries of the LCR	2.36	0.55	0.85	0.40	0.34	0.79	1.05	0.11	0.12	1.00	1.00
	Main stream and tributaries of the NR	2.01	0.55	0.99	0.22	0.42	0.94	2.27	0.03	0.12	1.01	1.00
Theoretical solutions	Main stream and tributaries of the YLZBR	7.58	0.43	0.50	0.12	0.44	0.70	1.11	0.14	0.45	1.01	1.00
	Minimum variance theory [34]		0.50			0.38			0.13			1.01
	Momentum diffusion [35]		0.50			0.42			0.08			1.00
	Minimum stream power [36]		0.47			0.42			0.11			1.00
	Threshold theory [37]		0.46			0.46			0.08			1.00
Global	72 streams around the world-range [4]		0.03–0.89			0.09–0.70			–0.51–0.75			
	72 streams around the world-model class [4]		0.4–0.5			0.3–0.4			0.1–0.2			

### 2.1.2. Data Collection

In situ-measured discharges and corresponding river widths, average flow depths, flow velocities, and cross sectional morphologies were all acquired from the Annual Hydrological Reports of P.R. China (1967–2019). As indicated by Qin et al. [7], the dataset

covers a wide range of stream patterns, which have high representation of the rivers in this area. Sixty cross sections were located within the area of the QTP, while another 69 cross sections were located outside the southeastern and northeastern margins of the QTP. The HydroSHEDS River Network (<https://www.hydrosheds.org/page/hydrorivers>, accessed on 31 May 2023) was used as a basic dataset to locate the in situ-measured cross sections.

### 2.1.3. Data Screening

The total number of cross sections with long-term measurements was 209, and 129 cross sections were selected for study. The criteria for selecting the cross sections were as follows: (1) having a consecutive hydrological record exceeding 10 years; (2) experiencing relatively low anthropogenic influence (e.g., no hydropower station and artificial diversion 10 km upstream and downstream of the measured cross section; located outside the backwater zone of a dam) during the study time period to minimize the external disturbance; (3) located at a distance from the regions that might be affected by extreme events such as landslides, debris flows, and glacial outbursts; (4) for cross sections that experienced notable bed elevation changes greater than 1 m between years, we took into account data with evident deposition or scouring and removed them from the following analysis; and (5) acting as a natural riverway with perennial drainage [7].

While alluvial reaches and bedrock-constrained reaches alternated with transient reaches in the rivers we studied, the selected cross sections were predominantly located in alluvial reaches, which were deemed more favorable for establishing hydrological stations. These reaches, which were in the quasi-equilibrium state, were characterized by a stable morphology and exhibited relatively minor fluctuations in erosion and sediment deposition both within and between years. Therefore, the relationships between water level and discharge were found to be curves rather than loops. The bed and bank materials of these cross sections are similar and mainly consist of gravel and sand. Table S1 shows a qualitative description of the bed and bank materials of the 129 studied cross sections.

## 2.2. Estimation of Discharges Based on Different Frequencies and Bankfull Conditions

### 2.2.1. Estimation of Discharges Based on Different Frequencies/Recurrence Intervals

Annual maximum peak discharges (over no less than 20 years) of each cross section were used to quantify discharge–frequency relations via Pearson III curves. For each cross section, the corresponding discharges from a 95.2% discharge frequency (equal to a recurrence interval of 1.05) to the minimal discharge frequency (equal to the recurrence interval of bankfull discharge) of a studied cross section group were estimated. Using the Huangshui River (Figure 1 and Table 2) as an example, there were five consecutive cross sections in this river reach (the number of cross sections per river reach in this study ranged from 1 to 11). The recurrence intervals of these cross sections (cross section IDs 20–24 in Table S1) under bankfull conditions were 2.28, 2.58, 2.34, 2.16, and 2.34, respectively. The value of the minimal recurrence interval under bankfull conditions for all cross sections of the Huangshui River cross section group was 2.16. Therefore, discharges of the recurrence intervals of 1.05, 1.10, 1.15, 1.20, 1.30, . . . , 2.0, 2.1, 2.16 for the five cross sections were estimated.

### 2.2.2. Estimation of Bankfull Discharge

There are two primary ways to define the bankfull discharge: one is based on the discharge frequency or flow duration; the other is based on the river cross section morphology [1].

To illustrate the estimation based on cross section morphology, the morphologies of 129 cross sections were first depicted to detect turning points (Figure 2). The potential bankfull positions (turning points) of each cross section were recorded if an evident break or discontinuity existed (Figure 2). In detail, bed elevation was in situ measured for every 1 m to the left bank. The indicator  $\alpha$  is defined as the elevation change rate:  $\alpha_i = (|h_{i+1} - h_i|)/h_i$ , where  $i = 0, 1, 2, \dots, n$  is the distance to the left bank, and  $h_i$  is the bed elevation at the  $i$ th distance to the left bank (m). If  $\alpha_i > 20\%$ , then the first point from the left bank at the  $i$ th distance was defined as a potential bankfull position. If

$\alpha_i \leq 20\%$ , then the point at the  $i$ th distance to the left bank was recognized as an integral part of the river bed or river bank. Then, the discharge frequencies of the potential bankfull positions were checked to determine whether they met general requirements. Potential bankfull positions with a recurrence interval of more than 8 years were removed [38]. The determined bankfull turning point and corresponding bed elevation (equals to water level) were recorded. Discharge corresponding to bankfull water level was then determined based on the in situ-measured records or water level–discharge curve.

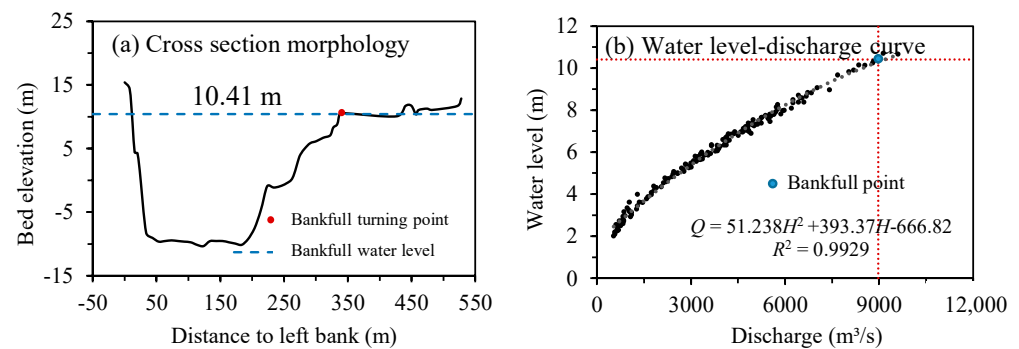


**Figure 2.** Typical cross section morphology (a), Nuxia cross section located at the main stream of the YLZBR), and corresponding water level–discharge rating curve (b).

Estimation for cross sections that have no evident flood plain (represented by the above-mentioned turning point) should account for the following factors: stream order, contributing area, upstream and downstream relationships, and main stream and tributary relationships. Previous studies have indicated that bankfull floods are often associated with a nearly constant discharge frequency (often in the range of 1–2 years) [39,40]. Therefore, the main steps in the estimation procedure are as follows: (1) use the mean of known bankfull discharge frequencies in the same river reach to impute the bankfull discharge frequencies of cross sections with unknown values; (2) if there is no known bankfull discharge frequency in the same reach, use the bankfull discharge frequency of the same stream order as an imputed value; (3) check the bankfull discharge of the frequencies determined by the above two steps using the Pearson III discharge–frequency curve; (4) the estimation is reliable if the bankfull discharge increases from upstream to downstream, and if this is not the case, check whether the discharge increases downstream and the cross section is influenced by evident anthropogenic disturbances, such as water divisions or reservoirs.

### 2.3. Calculation of DHGs under Different Discharge Frequencies and Bankfull Conditions

In situ-measured hydrological data with recurrence intervals equal to and less than the bankfull discharge were used to calculate DHGs. Bankfull discharge is the turning point at which the dynamic action of water and sediment transitions from shaping river channels to shaping floodplains. It dominates the shaping of river morphology as a reference discharge. Due to the sudden widening of a cross section above the bankfull water level, the morphology of the flood plain is evidently different from that of the main channel. Therefore, this study mainly focused on DHGs below bankfull water levels.

In situ-measured  $Q$ ,  $W$ ,  $H$ , and  $V$  under bankfull conditions and of the same discharge frequency were first sorted within the same group. Then, we fitted the DHG relations under bankfull conditions and different discharge frequencies. Two cases were considered (Figure 1 and Table 2): the same river reach and different reaches located in the same river basin. For the reaches with  $\geq 5$  cross sections, the width-, depth- and velocity-DHG of different discharge frequencies were fitted along the reach (Figure 1 and Table 2). For reaches with  $< 5$  cross sections, cross sections located in both the main stream and tributaries of a river basin were used to fit the DHG relations (different reaches located in the same river basin in Figure 1 and Table 2).

### 3. MFDHG Relations

#### 3.1. From DHG to MFDHG

DHG quantifies the relationship between a reference discharge (usually represented by channel-forming discharge or bankfull discharge) and the corresponding hydraulic variables of multiple cross sections. For a particular cross section, one reference discharge corresponds to only one river width, average flow depth, and flow velocity. This leads us to ask how the hydraulic variables of multiple cross sections would change with multiple water levels (discharge frequencies) across the watershed. The AMHG considers both the spatial connections of individual cross sections and multiple discharge frequencies. Another question is whether an AMHG-like relationship exists when DHG is the basis.

Based on the above hypotheses, we explored the relations among DHGs at multiple discharge frequencies to fully capture the variations in  $W$ ,  $H$ ,  $V$ , and  $Q$  across the river network. The intent was to promote the scientific understanding of HGs by identifying a previously unnoticed correlative relationship between a river's DHG coefficients and their corresponding exponents. This was achieved by plotting  $a$ - $b$ ,  $c$ - $f$ , and/or  $k$ - $m$  DHG pairs for multiple temporally distributed discharge frequencies, for example, from thousands of in situ measurements of  $Q$ ,  $W$ ,  $H$ , and  $V$  collected from 1967–2019 at 129 cross sections located at national hydrological stations. Because these correlations were obtained by simply aggregating DHG parameter pairs from many discharge frequencies, they are here referred to as MFDHGs.

#### 3.2. Two Presentations of MFDHG

Similar to AMHG, the MFDHG correlation is driven by two facts: one is the mathematical construct with DHG exponents in both the regressor and the regressand, and the other is geomorphological coevolution among discharge, cross sectional shape, and hydraulic variables [41,42]. This paper defines the MFDHG from two aspects: mathematical expression, and geomorphological significance. It is noteworthy to state that only DHGs with  $R^2 > 0.5$  were considered for the construction of MFDHGs, thereby ensuring the reliability and accuracy of the analysis.

##### (1) MFDHG expressed as log-linear relations between DHG coefficients and exponents

Inspired by the idea of the AMHG, which relates AHG coefficients and exponents using a log-linear relation [12], we employed various functions, including linear, exponential, quadratic, and log-linear models, to fit the DHG coefficients and exponents. Our analysis revealed that the log-linear function demonstrated the most promising results, thus enabling the definition of the MFDHG:

$$b = \alpha_1 \ln(a) + \beta_1 \quad (4)$$

$$f = \alpha_2 \ln(c) + \beta_2 \quad (5)$$

$$m = \alpha_3 \ln(k) + \beta_3 \quad (6)$$

where  $\alpha_1$ ,  $\alpha_2$ , and  $\alpha_3$  are slopes of the MFDHG, and  $\beta_1$ ,  $\beta_2$ , and  $\beta_3$  are intercepts of the MFDHG.

Exponents  $b$ ,  $f$ , and  $m$  were shown to be functions of coefficients  $a$ ,  $c$ , and  $k$ , which reduced the number of unknown parameters in the DHG system by half. This feature also suggested that the DHG is not temporally specific, as previously theorized [3], but rather is dependent on the DHG of other discharge frequencies in a given river reach or different reaches in the same river basin. This also showed that MFDHG is not contradictory to the findings of DHG research over the past few decades, as suggested by a previous empirical analysis.

##### (2) MFDHG expressed as congruent hydraulics

MFDHG is a function of the integral geomorphology of a river basin. We found that MFDHG appeared when individual DHG rating curves for each discharge frequency in

a given river reach or at different reaches in the same river basin converged at the same values of  $W/H/V$  and  $Q$  (Figure S1); this relation is presented as the congruent hydraulic pairs  $Q_{cW} - W_c$ ,  $Q_{cH} - H_c$ , and  $Q_{cV} - V_c$ :

$$W_c = a_{p_1, p_2, \dots, p_x} Q_{cW}^{b_{p_1, p_2, \dots, p_x}} \quad (7)$$

$$H_c = c_{p_1, p_2, \dots, p_x} Q_{cH}^{f_{p_1, p_2, \dots, p_x}} \quad (8)$$

$$V_c = k_{p_1, p_2, \dots, p_x} Q_{cV}^{m_{p_1, p_2, \dots, p_x}} \quad (9)$$

where subscripts  $p_1, p_2 \dots p_x$  are temporally indexed discharge frequencies for all cross sections in a certain study area; subscript  $c$  is termed “congruent hydraulics”, the empirically fit parameters that define the MFDHG; and  $Q_{cW}$ ,  $Q_{cH}$ ,  $Q_{cV}$ ,  $W_c$ ,  $H_c$ , and  $V_c$  are congruent hydraulics determined by the internal geomorphic characteristics of a river basin. When plotting all DHG curves of a river under different discharge frequencies on the same coordinate system, an interesting phenomenon is observed—all the curves intersect at a single point (Figure S1), resulting in a convergence within the log-linear hydraulic coordinate space. These points of intersection represent congruent hydraulic pairs, indicating a consistent relationship between hydraulic parameters across various flow conditions.

Similar to the AMHG, congruent hydraulics for the MFDHG can be estimated by the intercepts and slopes of the MFDHG. Taking width-MFDHG as an example (Equation (7)), if any two discharge frequencies ( $p_1, p_2$ ) share  $W_c$  and  $Q_{cW}$ , then we can solve Equation (1) for  $W_c$  at each discharge frequency and equate the two expressions:

$$b_{p_1} \log(Q_{cW}) + \log(a_{p_1}) = b_{p_2} \log(Q_{cW}) + \log(a_{p_2}) \quad (10)$$

Moving  $Q_{cW}$  to the left side of the equation gives the slope ( $\alpha_1$ ) of the MFDHG by two cross sections:

$$-\frac{1}{\log(Q_{cW})} = \frac{b_{p_2} - b_{p_1}}{\log(a_{p_2}) - \log(a_{p_1})} = \alpha_1 \quad (11)$$

Finally, the intercept ( $\beta_1$ ) of MFDHG can be defined empirically as

$$\beta_1 = \frac{\log(W_c)}{\log(Q_{cW})} \quad (12)$$

Ideally, based on Equations (11) and (12), congruent values of  $Q_{cW}$  and  $W_c$  for multiple discharge frequencies can be estimated. However, MFDHG slopes and intercepts for any two discharge frequencies are not equal in actual river systems. Congruent hydraulics estimated based on any two discharge frequencies are also not equal. Therefore, the mean intercepts and slopes of all possible combinations of MFDHG slopes and intercepts should be used to estimate congruent hydraulics (e.g., if a given river reach has 20 DHGs under 20 discharge frequencies, this results in 190 slope and intercept pairs corresponding to 190 discharge frequencies). Subsequently, the mean slope and intercept of these 190 pairs were used to estimate the congruent hydraulics of the river reach.

## 4. Results

### 4.1. DHGs under Bankfull Conditions

The existence of DHG under bankfull discharge is a prerequisite for the further study of MFDHG. Four river reaches were used to study DHGs along a river reach (Figure 1). The main streams of the Lantsang River, the upper Yellow River, and its tributary, the Huangshui River, exhibited relatively strong DHGs with  $R^2 > 0.5$  (Table 2). The DHG of the Jinsha River was weak overall, which may be attributed to the influence of the braided Tuotuo River reach. A relatively large bed slope and  $W$ , as well as small  $Q$  and  $H$  values, weakened the consistent adjustments of  $W$ ,  $H$ , and  $V$  to  $Q$  variations (Table 2).

Five river basins, including both the main stream and tributaries, were used to study the DHGs of different reaches located in the same basin (Figure 1 and Table 2). Generally, the DHG strengths of different reaches located in the same river basin were weaker than those along a single river reach. In particular, the DHG strengths of tributaries of the Yalong River were nearly the weakest among all scenarios. Data from cross sections located within 10 km upstream and downstream of hydropower stations and artificial diversions were removed through data screening processes. However, large-scale hydropower development and construction projects (22 cascade hydropower stations along the 1571 km main stream) still contributed to changes in the discharge–sediment relationship and further to the weak DHG relations. The shaping of river morphology was no longer dominated by natural discharge–sediment processes but was largely influenced by artificial runoff regulation. Adjustments of  $W$ ,  $H$ , and  $V$  to  $Q$  were impaired, and the DHG relation was weakened.

The cross section morphology is shaped by discharge and sediment load and influenced by boundary conditions such as geology and geomorphology [43]. Variations in climate and underlying surfaces are smaller within one river basin than across basins, which results in a strong correlation between discharge and hydraulic variables in one basin. This provides a basis for studying the MFDHG for different reaches located in the same river basin and emphasizes the importance of similar boundary conditions under regime theory in HG studies.

Although within the range ( $-0.51$ – $0.75$ ) proposed by Park [4] for 72 streams around the world, the velocity exponent  $m$  of the Lantsang River was  $<0$ , which is rare (Table 2). In addition, the DHG exponents of our research showed relatively large differences compared to the four theoretical solutions presented in Table 2. This may be attributed to the fact that DHG relations may not be observed in steep mountain streams unless certain criteria, such as stream power/grain size threshold standards, are met [44]. We did not verify the standards proposed by Wohl and Wilcox [44], but the results confirmed the existence of DHGs in the study area, which supports the exploration of the relationships of DHGs under multiple discharge frequencies and the development of the MFDHG concept.

#### 4.2. MFDHG under Different Scenarios

To verify the hypotheses proposed in Section 3, we tested the MFDHG relations in two sets of data obtained along a single river reach and from different river reaches located in the same river basin (Figure 1 and Table 2).

##### 4.2.1. MFDHG along a River Reach

DHG coefficients and exponents under multiple discharge frequencies showed good log-linear correlations along the river reaches. The determination coefficients  $R^2$  of MFDHG along the four river reaches were  $>0.82$  (Figure 3 and Table 3). Depth-MFDHGs exhibited the strongest correlations, while width- and velocity-MFDHGs had lower strengths (Table 3). Analytically, depth was more responsive in adjusting to accommodate changes in discharge and stream power, while width may have been more prone to random variations in boundary conditions such as geologic constraints and human modifications [41]. Variations in the velocity exhibited relatively strong randomness and less consistency. The slopes of mountain rivers changed significantly along different reaches; as a result, the regularity of velocity change along the reach was not sensitive. This led to a nonsignificant adjustment in velocity with variable discharge and low exponents  $m$  and  $R^2$  of MFDHG. Furthermore, the MFDHG slopes of the three major rivers (Yellow River, Jinsha River, Lantsang River) were smaller than that of the tributary Huangshui River (Figure 3).

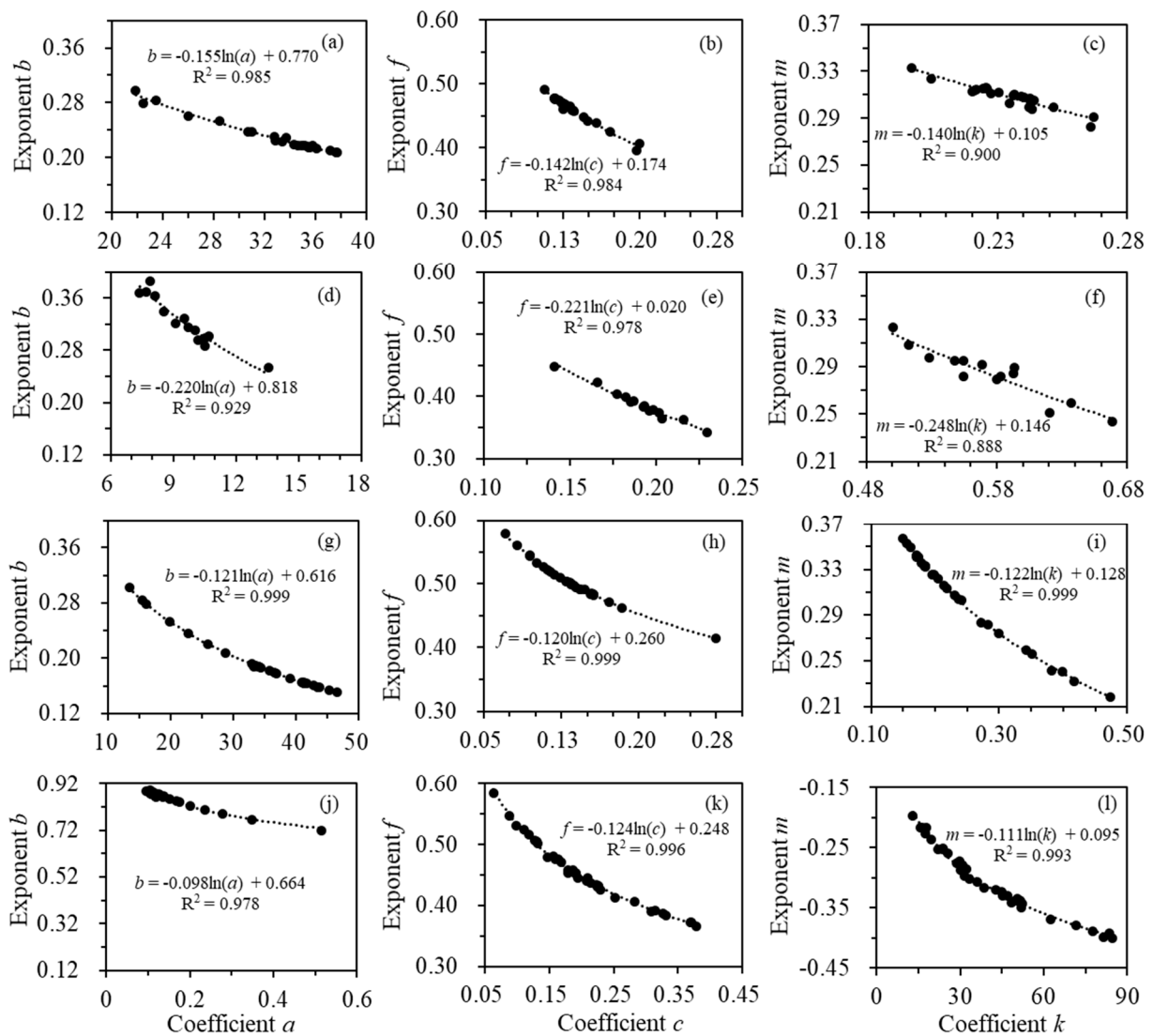


**Figure 3.** Relations between DHG coefficients and exponents at multiple discharge frequencies for the main streams of the upper YR (a–c), Huangshui River (d–f), upper JSR (g–i), and LCR (j–l). As an example, subfigure (a) encompasses data from cross sections 2 through 12 (Table S1). Width-DHG relationships for discharge frequencies of 5%, 10%, 15%, ..., 95% were first fitted. Then, a total of 20 pairs of DHG coefficients and exponents was determined and utilized to generate the MFDHG relation.

The strength  $R^2$  of the MFDHG was determined by the degree of DHG curve convergence in double logarithmic coordinate systems [27].  $R^2$  can be interpreted as a geomorphic index indicating the variability of water surface morphologies for different discharge frequencies (taking width-DHG as an example) and the hydraulic self-similarity of a certain study area. Both the log-linear relations between DHG coefficients and exponents and the convergence of DHG rating curves reflected hydraulic self-similarity and consisted of variations in channel morphology, which enabled the extraction of DHG common features and the achievement of an overall HG. In addition, the strong MFDHG correlations also indicated the equilibrium state of the studied river reaches, which could be reflected by the similar boundary sediments of the studied cross sections (Table S1).

**Table 3.** Z-values of the Mann–Kendall test in detecting changes in DHG coefficients and exponents with discharge frequency and strengths  $R^2$  of MFDHG along a river reach and different reaches in the same river basin. The number of asterisks represents the level of significance: \* is 0.05, \*\* is 0.01, and \*\*\* is 0.001.  $|Z| > 1.96$ ,  $|Z| > 2.58$ , and  $|Z| > 3.30$  indicate that the trends are significant at the  $\alpha = 0.05$ ,  $\alpha = 0.01$ , and  $\alpha = 0.001$  levels, respectively. The positive and negative signs indicate increasing and decreasing trends in the time series, respectively.  $R^2$  indicates the determination coefficient between DHG coefficients and exponents.

Sources	Scenarios	Mann–Kendall Test Z		$R^2$ of Width-MFDHG	Mann–Kendall Test Z		$R^2$ of Depth-MFDHG	Mann–Kendall Test Z		$R^2$ of Velocity-MFDHG	Mean $R^2$ of MFDHG
		<i>a</i>	<i>b</i>		<i>c</i>	<i>f</i>		<i>k</i>	<i>m</i>		
Along a river reach	Main stream of the YR	1.44 *	−1.93 **	0.985	−2.68 ***	2.68 ***	0.984	0.40	0.74	0.900	0.956
	Main stream of the JSR	5.01 ***	−5.01 ***	0.999	0.09	−0.17	0.999	−4.15 ***	4.11 ***	0.999	0.999
	Main stream of the LCR	−5.43 ***	3.49 ***	0.978	−1.92 **	2.16 **	0.996	5.14 ***	−4.70 ***	0.993	0.989
	Main stream of the Huangshui River	1.98 **	−2.08 **	0.929	−0.40	0.49	0.978	−1.78 **	2.47 ***	0.888	0.932
	Mean			0.973			0.989			0.945	0.969
Different reaches located in the same river basin	Tributaries of the JSR	−0.53	−3.01 ***	0.448	−1.32 *	2.27 **	0.928	1.74 **	−0.90	0.933	0.770
	Tributaries of the YLR	−3.66 ***	−0.06	0.511	−1.30 *	1.39 *	0.991	3.02 ***	−1.65 **	0.939	0.814
	Tributaries of the LCR	−7.56 ***	6.03 ***	0.932	0.51	1.40 *	0.761	5.60 ***	−3.74 ***	0.963	0.885
	Main stream and tributaries of the NR	−8.08 ***	7.66 ***	0.976	2.72 ***	−2.91 ***	0.972	3.89 ***	−2.66 ***	0.924	0.957
	Main stream and tributaries of the YLZBR	−2.45 ***	2.37 ***	0.993	1.75 **	−2.71 ***	0.944	0.14	1.02	0.833	0.923
Mean			0.772			0.919			0.918	0.870	
Mean			0.861			0.950			0.930	0.914	

#### 4.2.2. MFDHG for Different Reaches Located in the Same River Basin

The MFDHG strengths for different reaches located in the same river basin were high but were generally lower than those along the same reach (Figure 4 and Table 3). The mean  $R^2$  values for MFDHG along a river reach and on different reaches in the same river basin in this study were 0.969 and 0.870 (Table 3), respectively, suggesting that rating curve convergence was widespread in our data. Similar to the observations from AMHG research [41], width-MFDHG strength with a mean  $R^2$  of 0.861 arose mainly from the mathematical construct, had only weak geomorphological significance, and was weaker than those of depth- and velocity-MFDHG (with mean  $R^2$  values of 0.950 and 0.930, respectively), which were dominated by geomorphological coevolution (Table 3).

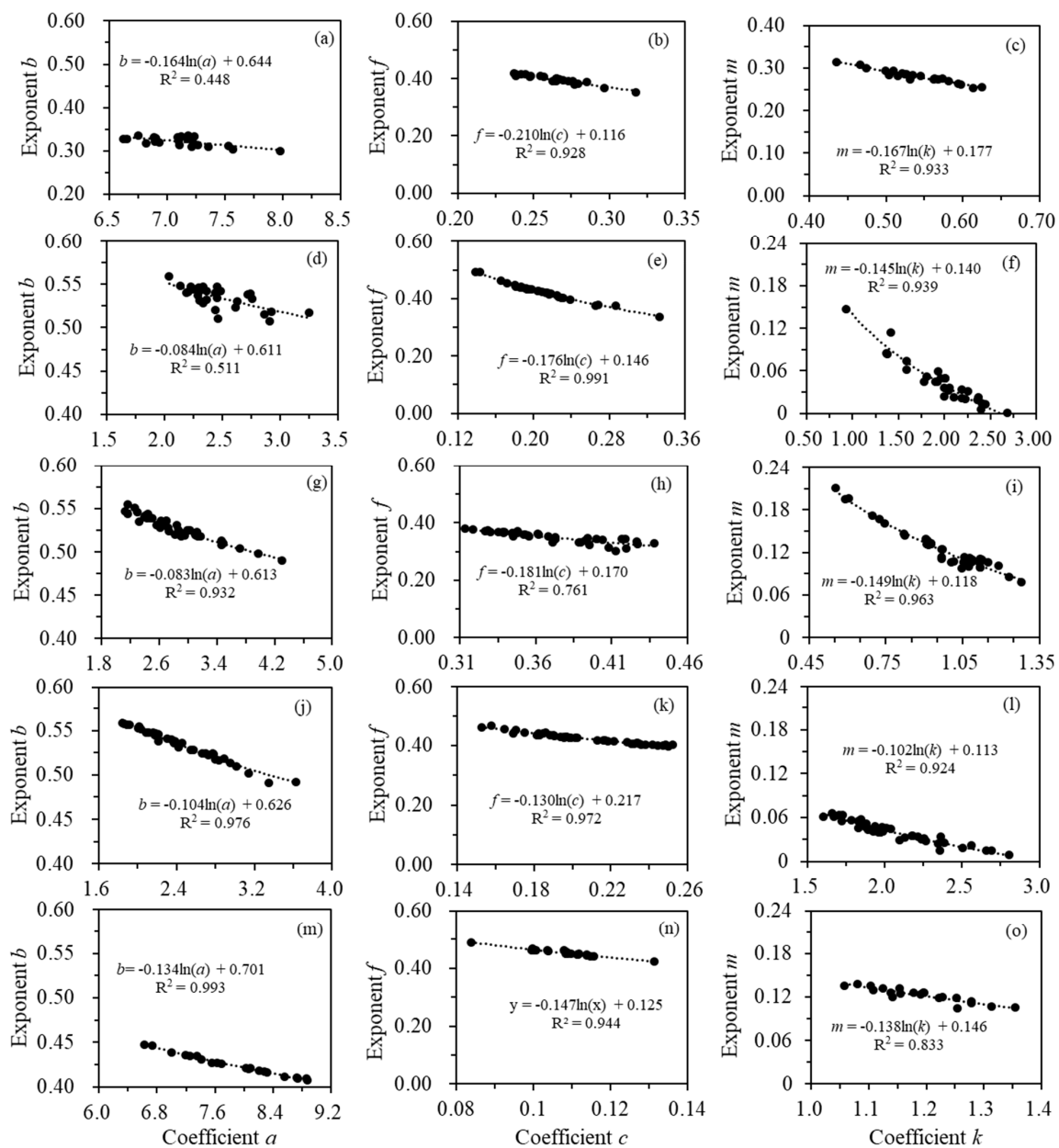


**Figure 4.** Relations between DHG coefficients and exponents at multiple discharge frequencies for tributaries of the JSR (a–c), tributaries of the YLR (d–f), tributaries of the LCR (g–i), the main stream and tributaries of the NR (j–l), and the main stream and tributaries of the YLZBR (m–o).

Correlations between DHG coefficients and exponents under multiple discharge frequencies reflected the spatial consistency of HG parameters in a certain study area. The

spatial continuity of water and sediment was strong along a river reach, which contributed to a greater MFDHG strength. The spatial heterogeneity of the geology and geomorphology of different river reaches was generally high, and the spatial continuities of discharge and sediment were lower than those along the same river reach. This contributed to the decrease in MFDHG strength for the scenario of different river reaches. Similar conclusions were introduced by Qin et al. [7], who extended the AMHG concept from the reach scale to the watershed scale. These authors noted that cross sections across river reaches showed strong AMHG relations, although weaker than those along a reach, which also reflects the consistency in flowing water and sediment as well as local climate, landscape, soil, vegetation, etc.

#### 4.3. Coordinated Variations in DHG Coefficients and Exponents

Correlations between DHG coefficients/exponents and discharge frequencies for nine scenarios were explored (Table 3). Coefficient  $a$  represents river widths for unit-width discharge along a reach. This reflects the ability of the unit-width flow to shape river morphology. Variations in river widths under unit-width discharge along a reach can be mainly attributed to variable boundary conditions. Exponent  $b$  represents the rate of increase in river width with increased discharge along the reach under a certain discharge frequency. This reflects the consistency of the shaping power of flowing water on river morphology.

Taking the main stream of the upper Yellow River as an example, exponent  $b$  decreased with increasing coefficient  $a$ , which could be expressed as a good log-linear relation with an  $R^2$  of 0.985 (Table 3 and Figure 5a). With increased discharge frequency, coefficient  $a$  and exponent  $b$  showed an increase and a decrease, respectively, but the variations with discharge frequency were not strictly one-to-one (Figure 5a–c). Specifically, with increasing discharge recurrence intervals, coefficients and exponents for width- and depth-MFDHG exhibited statistically significant variations (passed the M–K test at the 0.01 confidence level, Figure 5b,c,e,f), while a trend was not evident for velocity-MFDHG (Figure 5h,i). For the other eight scenarios, DHG coefficients and exponents exhibited the opposite variation trends with increasing discharge recurrence intervals if both passed the M–K test at the 90% confidence level (Table 3). For a coefficient and exponent pair that passed the 99% confidence level, the MFDHG strength varied from 0.920 to 0.999 with a mean of 0.974; if one of the coefficients or exponents did not pass at the 90% confidence level, the MFDHG strength varied from 0.448 to 0.999 with a mean of 0.795 (Table 3). Therefore, consistent variations in DHG coefficients and exponents with discharge frequency, represented by the M–K test Z-value, were one of the determinants of MFDHG strength.

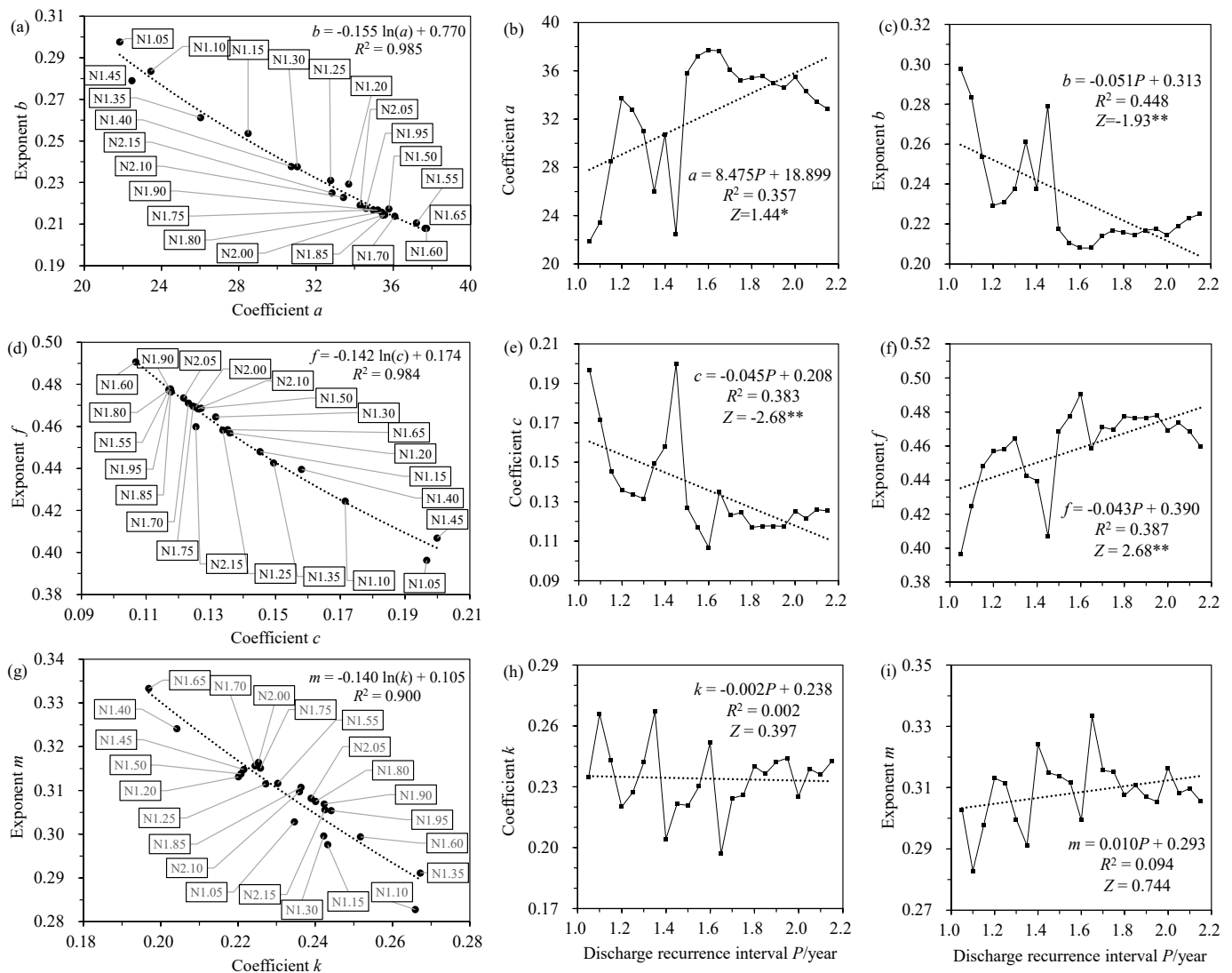


**Figure 5.** Relations between DHG coefficients and exponents (a,d,g) and their variations depending on discharge recurrence intervals (b,c,e,f,h,i) for the main stream of the upper YR. In subfigures (a,d,g), dashed lines represent the variation trends between DHG coefficients and exponents, and discharge recurrence intervals. N1.05 inside the black box of subfigure (a) represents the discharge recurrence interval is 1.05 years. In subfigures (b,c,e,f,h,i), solid polygons represent the values of DHG coefficients or exponents under different discharge recurrence intervals, dashed lines represent the variation trends between DHG coefficients and exponents, and discharge recurrence intervals, the number of asterisks represents the level of significance: \* is 0.05, \*\* is 0.01.

## 5. Discussion

### 5.1. Explanations of Congruent Hydraulics

A river reach exhibits a perfect MFDHG (with  $R^2 = 1$ ) when individual DHG rating curves converge exactly at a congruent point (Figure S1). Understanding the meaning and variation trends of congruent hydraulics contributes to revealing the physical basis of the MFDHG concept. Unlike AMHG research, which mainly focuses on short discharge-conserving reaches [27], the congruent hydraulics of MFDHG can be explained with the conceptual model in Figure 6 for relatively long reaches with tributaries. The flows used to generate the MFDHG in this study ranged from a 1.05-year recurrence interval to bankfull conditions (Sections 2.2 and 2.3), but in this section, the flow range is extended from extreme minimum to extreme maximum discharge to construct a conceptual model and fully illustrate the variations in hydraulic variables when  $P_c$ ,  $Q_c$ ,  $W_c$ , and  $H_c$  are requested:

- (1) Congruent discharge frequency ( $P_c$ ): for cross sections along a reach that share a  $P_c$  (e.g., 2.5 years recurrence interval discharge),  $Q$  and the corresponding  $W$ ,  $H$ , and  $V$  increase with increasing drainage area and confluence of tributaries (Figure 6a). This scenario can be described with DHG.
- (2) Congruent discharge ( $Q_{cW}/Q_{cH}/Q_{cV}$ ): for cross sections along a reach that share a  $Q_c$ , the value should be equal to both the discharge of one extreme flood event of the uppermost cross section and the discharge of one extreme low water event of the lowermost cross section. The probability of  $Q_c$  occurrence increases first and then decreases for cross sections along the reach (Figure 6b).
- (3) Congruent average flow depth ( $H_c$ ): for cross sections along a reach that share an  $H_c$ , river widths increase with the gradual change in cross sectional morphology from narrow V-shaped to wide U-shaped along the reach (Figure 6c).
- (4) Congruent river width ( $W_c$ ): for cross sections along a reach that share a  $W_c$ , average flow depths decrease along the reach (Figure 6d).

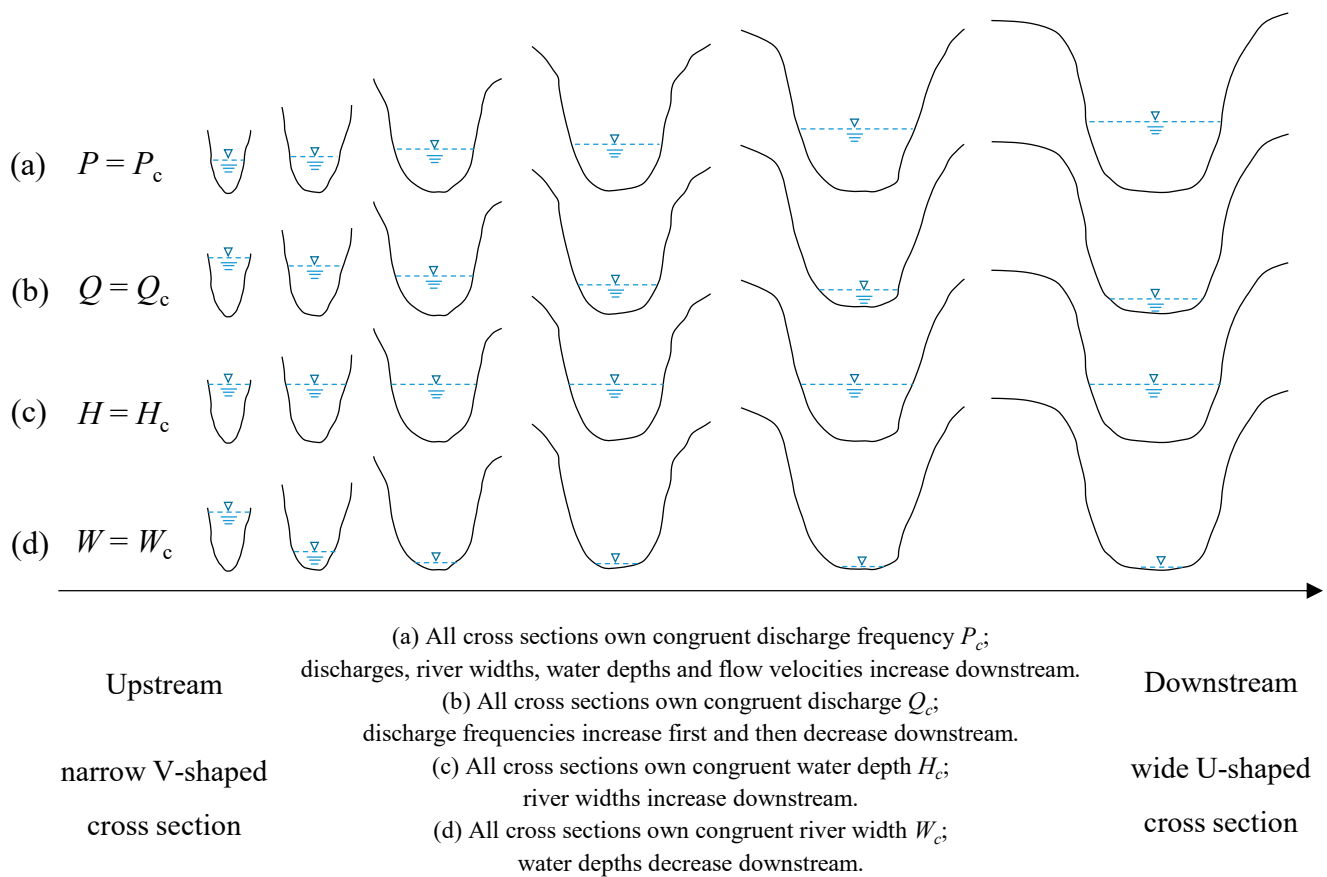


**Figure 6.** Conceptual model for congruent hydraulics of (a) DHG and (b–d) MFDHG.

$Q_{cW}$ ,  $Q_{cH}$ , and  $Q_{cV}$  represent three congruent discharges when the  $W$ ,  $H$ , and  $V$  of different cross sections are equal. These discharges may not be equal to each other or lie far outside the range of observed values given the very large variations in  $W$ ,  $H$ , and  $V$  downstream. Furthermore, the conceptual model can be extended for different river reaches located in the same river basin due to the dominant effects of flow and sediment processes on shaping river morphology. This dominant shaping effect can be maximized when river boundary sediments are similar and the river is in an equilibrium state, which usually occurs in lowland alluvial rivers or alluvial reaches of mountain rivers. The convergence of DHG curves indicates hydraulic self-similarity of river morphology in a certain study area induced by discharge and sediment load; this provides part of the theoretical basis for congruent hydraulic variables.

### 5.2. Significance of MFDHG for the HG System

Based on former studies of AHG, DHG, and AMHG [3,5,7,12,45], the concept of MFDHG, with respect to the sequence of temporal and spatial HG dimensions, has compensated for the shortcomings of a single DHG time dimension and the impossibility of describing consistent variations in hydraulic variables along a river reach under different discharge frequencies. MFDHG is practically useful because it is convincingly aligned with the actual character of the hydraulic geometry system. The relations among AHG, DHG, AMHG, and MFDHG in terms of temporal and spatial dimensions are outlined as follows (Figure 7):

- (1) DHG quantifies the spatial distributions of channel morphology shaped by channel-forming discharge (bankfull discharge). It reflects variations in hydraulic variable-discharge relations downstream of a reach or at different reaches located in the same river basin. Multiscale variations in river morphology in the spatial dimension can be depicted by DHG, but the time dimension has only one scale.
- (2) AHG quantifies the morphological characteristics of a single cross section under different discharge frequencies. It reflects variations in hydraulic variable-discharge relations for individual cross sections and depicts multiscale changes in cross sectional morphology in the temporal dimension, but the spatial dimension has only one scale.
- (3) AMHG relates the AHG of different cross sections along a river reach and extends the one-dimensional AHG in space. A multidimensional spatiotemporal connection between the geometric parameters of the cross section and discharge is reflected.
- (4) MFDHG extends the multiscale spatial attributes of DHG in the temporal dimension and contributes to achieving the same goal of relating river morphological parameters and discharges in both spatial and temporal dimensions.

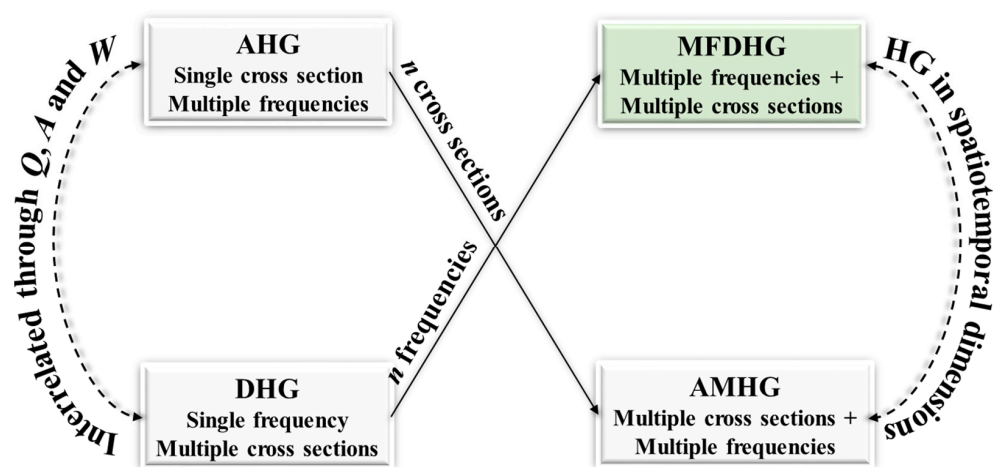


**Figure 7.** Mutual transformations among AHG, DHG, AMHG, and MFDHG. AHG and DHG can be linked through discharge  $Q$ , drainage area  $A$ , and river width  $W$  [26].

Since DHG relies on bankfull variables at a cross section and cross sectional shape (which determines AHG) determined by bank strength and sediment transport properties, DHG and AHG are implicitly linked [28]. For an ideal channel whose riverbanks and bed are composed of homogeneous noncohesive material, the channel morphology adjusts readily to changes in discharge, and the AHG and DHG do not differ [29]. A natural river may scale consistently with flow and sediments in the AHG and DHG if the river is in an equilibrium state and within the constraints of similar channel-bounding materials [46]. Previous studies have shown that strong AHG and AMHG relations exist in disconnected alluvial reaches of mountain rivers located in the QTP [6,7]. This paper focuses on these alluvial reaches and verifies the dominant role of the power conveyed by water and sediment in shaping river morphology. The alluvial characteristics of mountain rivers can be characterized by the existence of DHG and the coordinated variations in DHG coefficients

and exponents of the disconnected alluvial reaches. Therefore, for a natural alluvial river or an alluvial reach located in a mountain river, common features can be extracted from both the AHG and DHG, which provides a basis for the study and interpretation of the AMHG and MFDHG.

### 5.3. Differences and Relations between AMHG and MFDHG

Based on the above analysis, the main differences between MFDHG and AMHG can be summarized as follows:

- (1) Focus: AMHG examines the relationships between AHG coefficients and exponents, whereas MFDHG explores the relationships between DHG coefficients and exponents.
- (2) Spatial and temporal extension: AMHG extends the one-dimensional AHG concept to spatial scales by considering different cross sections within a river. In contrast, MFDHG extends the one-dimensional DHG concept to temporal scales by capturing variations in hydraulic properties over different discharge frequencies.
- (3) Sequence of consideration: MFDHG and AMHG differ in the order of considering cross sections and discharge frequencies. MFDHG first considers spatial properties (cross sections) and then incorporates temporal properties (discharge frequencies), while AMHG follows the opposite order.

Congruent hydraulics serve as a representation of shared characteristics within a group of studied cross sections, allowing for the characterization of the relationships between MFDHG and AMHG. The question at hand is whether the congruent hydraulics observed in AMHG and MFDHG represent two distinct approaches to capturing the same phenomenon. Taking the upper Yellow River and the Jinsha River as examples, we found that the fitted correlations between HG coefficients and exponents exhibited similar trends (Figure 8), e.g., fitted lines of depth-AMHG and depth-MFDHG of the Jinsha River showed nearly the same trend, although the MFDHG line occupied only a short portion of the AMHG line. Downstream adjustments of  $W$ ,  $H$ , and  $V$  with  $Q$  were often smaller than those of individual cross sections. Specifically, the variations in  $Q$ ,  $W$ ,  $H$ , and  $V$  used to fit the DHG and MFDHG relations were 9.8–2830 m<sup>3</sup> s<sup>-1</sup>, 42.8–272 m, 0.51–7.21 m, and 0.45–3.45 m s<sup>-1</sup>, respectively. The variations in  $Q$ ,  $W$ ,  $H$ , and  $V$  used to fit the AHG and AMHG relations were 5.2–3590 m<sup>3</sup> s<sup>-1</sup>, 11–346 m, 0.4–6.1 m, and 0.14–6.53 m s<sup>-1</sup>, respectively. In addition, we calculated the congruent hydraulics based on AMHG and MFDHG. The results showed that the relative differences in congruent hydraulics estimated by AMHG and MFDHG showed small differences and were within the range of 1.5–48.0% (Table 4). River width-related congruent hydraulics,  $\log(Q_{cW})$  and  $\log(W_c)$ , showed the smallest relative difference. The similar AMHG and MFDHG trend lines and small relative difference of AMHG and MFDHG congruent hydraulics indicated that the spatiotemporal characteristics of HG can be interpreted by either the AMHG or the MFDHG. This might contribute to the establishment of an overall HG.

**Table 4.** Congruent hydraulics calculated by AMHG and MFDHG of the Yellow River and the Jinsha River.

River Systems	HG Types	$\log(Q_{cW})$	$\log(Q_{cH})$	$\log(Q_{cV})$	$\log(W_c)$	$\log(H_c)$	$\log(V_c)$
Yellow River	AMHG	6.8	7.8	8.3	5.3	1.4	1.3
	MFDHG	6.3	7.4	7.0	4.9	1.4	0.7
	Relative difference (%)	8.1	5.9	16.1	6.3	2.0	48.0
Jinsha River	AMHG	7.3	10.5	7.5	5.1	2.8	0.7
	MFDHG	8.2	8.4	8.2	5.1	2.2	1.0
	Relative difference (%)	10.9	20.2	8.3	1.5	22.6	36.0

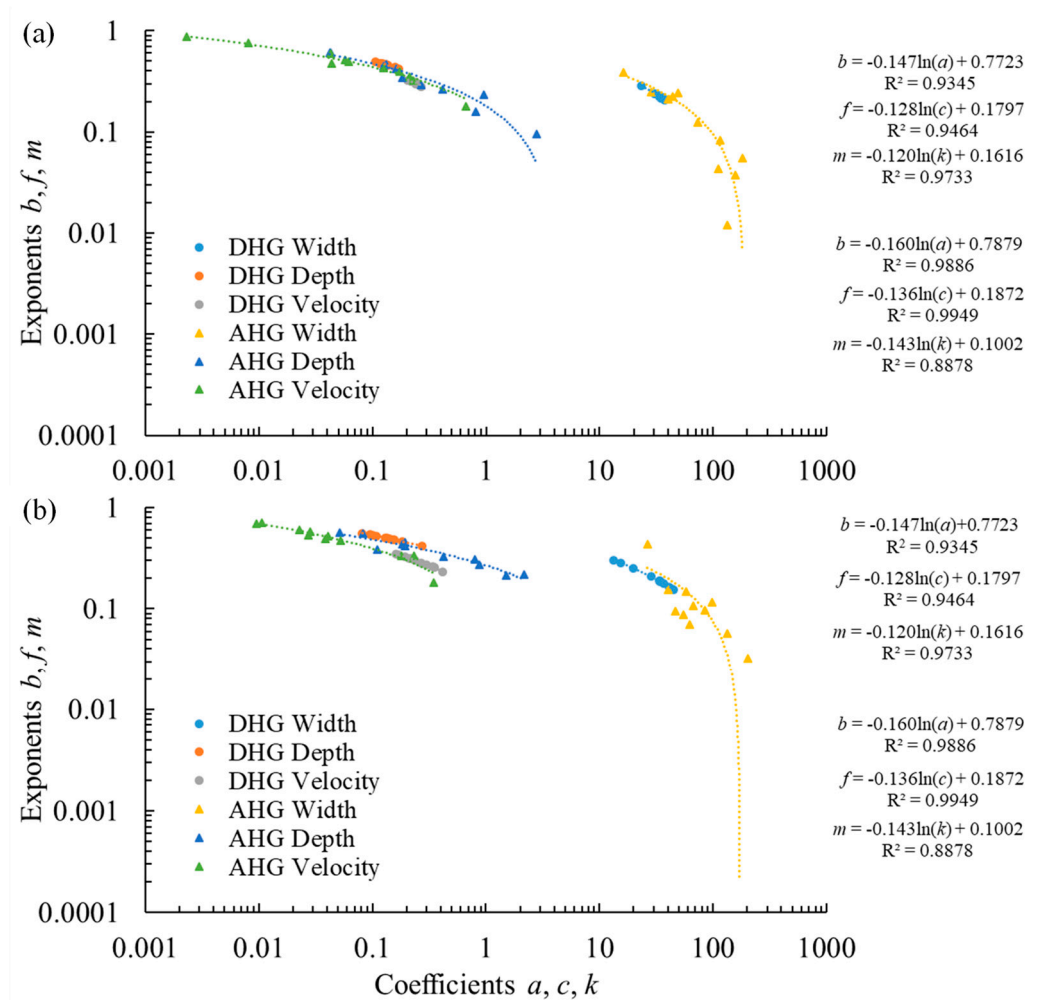


Figure 8. MFDHG and AMHG of the upper Yellow River (a) and the Jinsha River (b).

The overall HG relationship, although it has long been investigated by researchers [11,12,23,25], is expected to satisfactorily explain both AHG and DHG through AMHG and MFDHG. The ranges of applications of AHG and DHG are extended from the cross sectional scale and reach scale to the watershed scale by simultaneously considering multiple cross sections and discharge frequencies (Figure 7). Both AMHG and MFDHG are extensions of HG in the river network and reflect the applicability of hydraulic variable-discharge relations at the watershed scale. The concepts of AMHG and MFDHG provide methods and a theoretical basis for studying the spatial distributions of HG across river networks and reaching the goal of constructing an overall HG relationship.

## 6. Summary and Conclusions

Based on in situ measurements of six exoreic rivers and their tributaries originating from the QTP, this paper first verified the existence of DHGs in the study area, which is a prerequisite for studying MFDHGs, and then defined the MFDHGs according to mathematical expression and geomorphological significance. The MFDHG was finally verified both along a reach and for different reaches in the same river basin. The key findings and implications are as follows:

- (1) DHG, as a frequency-specific expression of hydraulics and channel geometry, appeared widely in the six major rivers and their tributaries that originate from the QTP.
- (2) The paired coefficients and exponents of DHG ( $a$  and  $b$ ,  $c$  and  $f$ , and  $k$  and  $m$ ) from multiple discharge frequencies along a given river reach or different reaches in the same

- river basin are functionally related to one another, exhibiting a log-linear relationship. This is the mathematical expression of MFDHG.
- (3) MFDHG, a mathematical construct arising from the use of power laws at a certain discharge frequency, is a novel geomorphic phenomenon after the discovery of AMHG. DHG rating curves reliably intersect at congruent  $Q_c$ ,  $W_c$ ,  $H_c$ , and  $V_c$ , indicating both geometric variability (to ensure rating curve intersection) and hydraulic self-similarity of river channels. This is the geomorphological expression of MFDHG.
  - (4) With increasing discharge frequency, the DHG coefficients and exponents showed opposite variations if both passed the M–K test at the 90% confidence level. Consistent variations in DHG coefficients and exponents with discharge frequency contributed to greater MFDHG strength.
  - (5) Although the empirical conclusion seemingly refutes previous decades of research defining DHGs as temporally independent, MFDHG relates individual DHGs under different discharge frequencies and contributes to the completeness of the HG system in terms of the spatiotemporal dimensions. This is a large step in refining the common features of DHG and will contribute to establishing an overall HG relationship considering multiple spatiotemporal dimensions across river reaches.
  - (6) Bed slope and bed material are important parameters that are adjusted based upon the incoming water and sediment. The future collection of additional data on bed slope, bed roughness, and materials in the study area using a combination of remote sensing, in situ measurements, and deep learning methods is proposed. These data can then be incorporated into the proposed MFDHG equations, further improving their accuracy and reliability.

**Supplementary Materials:** The following supporting information can be downloaded at <https://www.mdpi.com/article/10.3390/w15112139/s1>. Table S1: Cross sections studied in this research and their locations, slopes, upstream contributing areas, recurrence intervals of bankfull discharge, and bed/bank materials. Figure S1: Convergence of DHG curves of the main stream of the upper Yellow River (a–c), the main stream of the Huangshui River (d–f), the main stream of the upper Jinsha River (g–i), the tributaries of the Lantsang River (j–l), the main stream and the tributaries of the Nu River (m–o), and the main stream and the tributaries of the Yarlung Zangbo River (p–r) under multiple discharge frequencies. Red dots represent the congruent discharge, which indicates the convergence of individual DHG curves.

**Author Contributions:** Conceptualization, C.Q. and X.F.; data curation, Y.X. and G.W. (Ge Wang); funding acquisition, C.Q. and B.W.; methodology, C.Q.; software, Y.X. and G.W. (Ge Wang); validation, C.Q. and Y.X.; visualization, C.Q.; writing, review, and editing, C.Q., B.W., G.W. (Guangqian Wang) and X.F. All authors have read and agreed to the published version of the manuscript.

**Funding:** This research was funded by the Fund Program of the State Key Laboratory of Hydroscience and Engineering (2023-KY-02), the National Natural Science Foundation of China (Grant Nos. U2243218; U2243222; 52009061), the Postdoctoral Innovation Talents Support Program of China (Grant No. BX20190177), and the Shuimu Tsinghua Scholar Program (2020SM070).

**Data Availability Statement:** In situ-measured river width, average flow depth, flow velocity, and flow discharge data were provided by the Bureau of Hydrology at the Ministry of Water Resources of China, which is acknowledged here. These data can be sourced and made available from the Bureau of Hydrology at the Ministry of Water Resources of China (<http://www.mwr.gov.cn/english/>, accessed on 31 May 2023) upon reasonable request. Boundaries of the QTP are available at the National Tibetan Plateau Data Center (<http://www.tpdc.ac.cn/en/data/61701a2b-31e5-41bf-b0a3-607c2a9bd3b3/>, accessed on 31 May 2023). The SRTM 90 m DEM is available at <http://www.tpdc.ac.cn/en/data/23e32e3e-8104-4798-b7a1-325df8fd1a95/>, accessed on 31 May 2023.

**Conflicts of Interest:** The authors declare no conflict of interest.

## References

1. Eaton, B. Hydraulic geometry: Empirical investigations and theoretical approaches. In *Treatise on Geomorphology*; Academic Press: San Diego, CA, USA, 2013; pp. 313–329.
2. Lindley, E.S. Regime channels. *Proc. Punjab Eng. Congr.* **1919**, *7*, 63–74.
3. Leopold, L.B.; Maddock, T. *The Hydraulic Geometry of Stream Channels and Some Physiographic Implications*; U.S. Geological Survey Professional Paper 252; U.S. Government Printing Office: Washington, DC, USA, 1953.
4. Park, C.C. Worldwide variations in hydraulic geometry exponents of stream channels: An analysis and some observations. *J. Hydrol.* **1977**, *33*, 133–146. [[CrossRef](#)]
5. Lee, J.; Julien, P.Y. Downstream hydraulic geometry of alluvial channels. *J. Hydraul. Eng.* **2006**, *132*, 1347–1352. [[CrossRef](#)]
6. Qin, C.; Wu, B.; Wang, Y.; Fu, X.; Xue, Y.; Li, D.; Li, M.; Zhang, Y. Dynamic variability of at-a-station hydraulic-geometry for mountain rivers in the southeast Qinghai-Tibet Plateau: The cases of Yalong River and upper Jinsha River. *Catena* **2020**, *194*, 104723. [[CrossRef](#)]
7. Qin, C.; Wu, B.S.; Wang, G.Q.; Wang, G. Spatial distributions of At-Many-Stations Hydraulic Geometry for mountain rivers originated from the Qinghai-Tibet Plateau. *Water Resour. Res.* **2021**, *57*, e2020WR029090. [[CrossRef](#)]
8. Stall, J.B.; Yang, C.T. *Hydraulic Geometry of 12 Selected Stream Systems of the United States*; Research Report No. 32; University of Illinois Water Resources Research Center: Urbana, IL, USA, 1970.
9. Dingman, S.L.; Sharma, K.P. Statistical development and validation of discharge equations for natural channels. *J. Hydrol.* **1997**, *199*, 13–35. [[CrossRef](#)]
10. Parker, G.; Wilcock, P.R.; Paola, C.; Dietrich, W.E.; Pitlick, J. Physical basis for quasi-universal relations describing bankfull hydraulic geometry of single-thread gravel bed rivers. *J. Geophys. Res.* **2007**, *112*, F4005. [[CrossRef](#)]
11. Parker, G.; Wilkerson, G.V. Physical basis for quasi-universal relationships describing bankfull hydraulic geometry of sand-bed rivers. *J. Hydraul. Eng.* **2011**, *137*, 739–753.
12. Gleason, C.J.; Smith, L.C. Toward global mapping of river discharge using satellite images and at-many-stations hydraulic geometry-supporting data. *Proc. Natl. Acad. Sci. USA* **2014**, *111*, 4788–4791. [[CrossRef](#)]
13. Pelletier, J.D. Controls on the hydraulic geometry of alluvial channels: Bank stability to gravitational failure, the critical-flow hypothesis, and conservation of mass and energy. *Earth Surf. Dyn.* **2021**, *9*, 379–391. [[CrossRef](#)]
14. Song, X.; Zhong, D.; Wang, G.; Li, X. Stochastic evolution of hydraulic geometry relations in the lower Yellow River of China under environmental uncertainties. *Int. J. Sediment Res.* **2020**, *35*, 328–346. [[CrossRef](#)]
15. Andreadis, K.M.; Schumann, G.J.P.; Pavelsky, T. A simple global river bankfull width and depth database. *Water Resour. Res.* **2013**, *49*, 7164–7168. [[CrossRef](#)]
16. Bieger, K.; Rathjens, H.; Allen, P.M.; Arnold, J.G. Development and evaluation of bankfull hydraulic geometry relationships for the physiographic regions of the United States. *JAWRA J. Am. Water Resour. Assoc.* **2015**, *51*, 842–858. [[CrossRef](#)]
17. Rosgen, D.L. A classification of natural rivers. *Catena* **1994**, *22*, 169–199. [[CrossRef](#)]
18. Knighton, D. *Fluvial Forms and Processes*; Arnold: London, UK, 1998.
19. Wu, B.; Wang, G.; Xia, J.; Fu, X.; Zhang, Y. Response of bankfull discharge to discharge and sediment load in the Lower Yellow River. *Geomorphology* **2008**, *100*, 366–376. [[CrossRef](#)]
20. Hagemann, M.W.; Gleason, C.J.; Durand, M.T. BAM: Bayesian AMHG-Manning inference of discharge using remotely sensed stream width, slope, and height. *Water Resour. Res.* **2017**, *53*, 9692–9707. [[CrossRef](#)]
21. Raymond, P.A.; Zappa, C.J.; Butman, D.; Bott, T.L.; Potter, J.; Mulholland, P.; Laursen, A.E.; McDowell, W.H.; Newbold, D. Scaling the gas transfer velocity and hydraulic geometry in streams and small rivers. *Limnol. Oceanogr. Fluids Environ.* **2012**, *2*, 41–53. [[CrossRef](#)]
22. Raymond, P.A.; Hartmann, J.; Lauerwald, R.; Sobek, S.; McDonald, C.; Hoover, M.; Butman, D.; Striegl, R.; Mayorga, E.; Humborg, C.; et al. Global carbon dioxide emissions from inland waters. *Nature* **2013**, *503*, 355–359. [[CrossRef](#)]
23. Tabata, K.K.; Hickin, E.J. Interchannel hydraulic geometry and hydraulic efficiency of the anastomosing Columbia River, southeastern British Columbia, Canada. *Earth Surf. Process. Landf.* **2003**, *28*, 837–852. [[CrossRef](#)]
24. Rhodes, D.D. The b-f-m diagram: Graphical representation and interpretation of at-a-station hydraulic geometry. *Am. J. Sci.* **1977**, *277*, 73–96. [[CrossRef](#)]
25. Singh, K.P.; Broeren, S.M. Hydraulic geometry of streams and stream habitat assessment. *J. Water Resour. Plan. Manag.* **1989**, *115*, 583–597. [[CrossRef](#)]
26. Orlandini, S.; Rosso, R. Parameterization of stream channel geometry in the distributed modelling of catchment dynamics. *Water Resour. Res.* **1998**, *34*, 1971–1985. [[CrossRef](#)]
27. Gleason, C.J.; Wang, J. Theoretical basis for at-many-stations hydraulic geometry. *Geophys. Res. Lett.* **2015**, *42*, 7107–7114. [[CrossRef](#)]
28. Gleason, C.J. Hydraulic geometry of natural rivers: A review and future directions. *Prog. Phys. Geogr. Earth Environ.* **2015**, *39*, 337–360. [[CrossRef](#)]
29. Knighton, A.D. Variation in width-discharge relation and some implications for hydraulic geometry. *Geol. Soc. Am. Bull.* **1974**, *85*, 1069–1076. [[CrossRef](#)]
30. Chien, N.; Zhang, R.; Zhou, Z. *Fluvial Processes*; Science Press: Beijing, China, 1987.

31. Wolman, M.G. *The Natural Channel of Brandywine Creeck Pennsylvania*; U.S. Geological Survey Professional Paper; USGS: Reston, VA, USA, 1955; Volume 271, 56p.
32. Bray, D.I. Representative discharges for gravel-bed rivers in Alberta. *Canada. J. Hydrol.* **1975**, *27*, 143–153. [[CrossRef](#)]
33. Lewis, L.A. Some fluvial geomorphic characteristics of the Manati Basin, Puerto Rico. *Ann. Assoc. Am. Geogr.* **1969**, *59*, 280–293. [[CrossRef](#)]
34. Langbein, W.B. Geometry of river channels: Closure of discussion. *J. Hydraul. Div. Am. Soc. Civ. Eng.* **1965**, *91*, 297–313.
35. Parker, G. Hydraulic geometry of active gravel rivers. *J. Hydraul. Div. Am. Soc. Civ. Eng.* **1979**, *105*, 1185–1201. [[CrossRef](#)]
36. Chang, H.H. Geometry of gravel streams. *J. Hydraul. Div. Am. Soc. Civ. Eng.* **1980**, *106*, 1443–1456. [[CrossRef](#)]
37. Li, R.M.; Simons, D.B.; Stevens, M.A. Morphology of cobble streams in small watersheds. *J. Hydraul. Div. Am. Soc. Civ. Eng.* **1976**, *102*, 1101–1117. [[CrossRef](#)]
38. Williams, G.P. *Hydraulic Geometry of River Cross-Sections-Theory of Minimum Variance*; U.S. Geological Survey Professional Paper; U.S. Government Printing Office: Washington, DC, USA, 1978; Volume 1029.
39. Castro, J.M.; Jackson, P.L. Bankfull discharge recurrence intervals and regional hydraulic geometry relationships: Patterns in the Pacific Northwest, USA. *J. Am. Water Resour. Assoc.* **2001**, *37*, 1249–1262. [[CrossRef](#)]
40. Harvey, A.M. Channel Capacity and the Adjustment of Streams to Hydrologic Regime. *J. Hydrol.* **1969**, *8*, 82–98. [[CrossRef](#)]
41. Shen, C.; Wang, S.; Liu, X. Geomorphological significance of at-many-stations hydraulic geometry. *Geophys. Res. Lett.* **2016**, *43*, 3762–3770. [[CrossRef](#)]
42. Brinkerhoff, C.B.; Gleason, C.J.; Ostendorf, D.W. Reconciling at-a-station and at-many-stations hydraulic geometry through river-wide geomorphology. *Geophys. Res. Lett.* **2019**, *46*, 9637–9647. [[CrossRef](#)]
43. Wohl, E. *Mountain Rivers Revisited*; GEO Press: Washington, DC, USA, 2010.
44. Wohl, E.E.; Wilcox, A. Channel geometry of mountain streams in New Zealand. *J. Hydrol.* **2005**, *300*, 252–266. [[CrossRef](#)]
45. Wohl, E. Limits of downstream hydraulic geometry. *Geology* **2004**, *32*, 897–900. [[CrossRef](#)]
46. Eaton, B.C.; Church, M.; Millar, R.G. Rational regime model of alluvial channel morphology and response. *Earth Surf. Process. Landf.* **2004**, *29*, 511–529. [[CrossRef](#)]

**Disclaimer/Publisher’s Note:** The statements, opinions and data contained in all publications are solely those of the individual author(s) and contributor(s) and not of MDPI and/or the editor(s). MDPI and/or the editor(s) disclaim responsibility for any injury to people or property resulting from any ideas, methods, instructions or products referred to in the content.